



This is a repository copy of *DCP: A pipeline toolbox for diffusion connectome*.

White Rose Research Online URL for this paper:

<https://eprints.whiterose.ac.uk/209602/>

Version: Published Version

---

**Article:**

Huang, W. [orcid.org/0000-0002-2481-1188](https://orcid.org/0000-0002-2481-1188), Dong, X., Zhao, T. et al. (3 more authors) (2024) DCP: A pipeline toolbox for diffusion connectome. *Human Brain Mapping*, 45 (3). e26626. ISSN 1065-9471

<https://doi.org/10.1002/hbm.26626>

---

**Reuse**

This article is distributed under the terms of the Creative Commons Attribution-NonCommercial (CC BY-NC) licence. This licence allows you to remix, tweak, and build upon this work non-commercially, and any new works must also acknowledge the authors and be non-commercial. You don't have to license any derivative works on the same terms. More information and the full terms of the licence here: <https://creativecommons.org/licenses/>


**Takedown**

If you consider content in White Rose Research Online to be in breach of UK law, please notify us by emailing [eprints@whiterose.ac.uk](mailto:eprints@whiterose.ac.uk) including the URL of the record and the reason for the withdrawal request.



[eprints@whiterose.ac.uk](mailto:eprints@whiterose.ac.uk)  
<https://eprints.whiterose.ac.uk/>

# DCP: A pipeline toolbox for diffusion connectome

Weijie Huang<sup>1,2,3</sup>  | Xinyi Dong<sup>1</sup> | Tengda Zhao<sup>1</sup> | Ludmila Kucikova<sup>3</sup> | Anguo Fu<sup>1</sup> | Ni Shu<sup>1</sup>

<sup>1</sup>State Key Laboratory of Cognitive Neuroscience and Learning, Beijing Normal University, Beijing, PR China

<sup>2</sup>School of Systems Science, Beijing Normal University, Beijing, PR China

<sup>3</sup>Department of Neuroscience, Sheffield Institute for Translational Neuroscience, Medical School and Insigneo Institute for in Silico Medicine, University of Sheffield, Sheffield, UK

## Correspondence

Ni Shu, State Key Laboratory of Cognitive Neuroscience and Learning, Beijing Normal University, Beijing 100875, PR China.  
Email: [nshu@bnu.edu.cn](mailto:nshu@bnu.edu.cn)

## Funding information

STI2030-Major Projects, Grant/Award Numbers: 2022ZD0213300, 2021ZD0200500; National Natural Science Foundation of China, Grant/Award Numbers: 32271145, 81871425, 2231200165, 210510238; China Scholarship Council; Fundamental Research Funds for the Central Universities, Grant/Award Number: 2017XTCX04; State Key Laboratory of Cognitive Neuroscience and Learning, Grant/Award Numbers: CNLYB2001, CNLZD2101

## Abstract

The brain structural network derived from diffusion magnetic resonance imaging (dMRI) reflects the white matter connections between brain regions, which can quantitatively describe the anatomical connection pattern of the entire brain. The development of structural brain connectome leads to the emergence of a large number of dMRI processing packages and network analysis toolboxes. However, the fully automated network analysis based on dMRI data remains challenging. In this study, we developed a cross-platform MATLAB toolbox named “Diffusion Connectome Pipeline” (DCP) for automatically constructing brain structural networks and calculating topological attributes of the networks. The toolbox integrates a few developed packages, including FSL, Diffusion Toolkit, SPM, Camino, MRtrix3, and MRICron. It can process raw dMRI data collected from any number of participants, and it is also compatible with preprocessed files from public datasets such as HCP and UK Biobank. Moreover, a friendly graphical user interface allows users to configure their processing pipeline without any programming. To prove the capacity and validity of the DCP, two tests were conducted with using DCP. The results showed that DCP can reproduce the findings in our previous studies. However, there are some limitations of DCP, such as relying on MATLAB and being unable to fixel-based metrics weighted network. Despite these limitations, overall, the DCP software provides a standardized, fully automated computational workflow for white matter network construction and analysis, which is beneficial for advancing future human brain connectomics application research.

## KEYWORDS

DCP, diffusion connectome, diffusion tensor imaging, dMRI, graph theory, structural connectivity, structure network, white matter

## 1 | INTRODUCTION

Diffusion-weighted magnetic resonance imaging (dMRI) is an important technique for noninvasively studying white matter connectivity

(Behrens & Sporns, 2012; Sporns, 2011). Using dMRI tractography, white matter architecture can be reconstructed and visualized (Descoteaux et al., 2009; Girard et al., 2014). Combined with graph theory, white matter networks enable researchers to not only identify regions of interest but also investigate how these regions interact. Compared with metrics like fractional anisotropy and mean diffusivity,

Weijie Huang and Xinyi Dong contributed equally to this work.

This is an open access article under the terms of the [Creative Commons Attribution-NonCommercial](https://creativecommons.org/licenses/by-nc/4.0/) License, which permits use, distribution and reproduction in any medium, provided the original work is properly cited and is not used for commercial purposes.

© 2024 The Authors. *Human Brain Mapping* published by Wiley Periodicals LLC.

they can capture the rich and dynamic interconnectivity of brain regions, provide a new and more comprehensive perspective to deeply understand how the human brain performs complex cognitive tasks (Passingham et al., 2002) and reveal the pathogenesis of neuropsychiatric diseases (Fornito et al., 2015; van den Heuvel & Sporns, 2019). For instance, studies using network analysis based on white matter networks found altered rich club organization in schizophrenia, as well as impaired inter-hemispheric connection and decreased connectivity within emotion-regulating hub regions in bipolar disorder (Fornito et al., 2015; van den Heuvel & Sporns, 2019). However, the process of constructing white matter networks using raw dMRI data and T1-weighted data involves several intricate steps, and complex graph theory needs to be mastered to perform network analyses. Therefore, the great technical difficulty for clinicians, nonexperts, and nontechnical users limits the exploration of human brain white matter and replication of previous dMRI studies.

To the best of our knowledge, there is no available tool that has both the function of constructing white matter networks and performing network analyses. Even though some software and packages have been developed to facilitate dMRI processing, they all have more or less shortcomings. These tools can be divided into categories according to whether they have a graphic user interface (GUI) and whether they provide a pipeline of batch processing. The first set of tools, such as Camino (Cook et al., 2006), MRtrix3 (Tournier et al., 2019), Dipy (Garyfallidis et al., 2014), and QSIprep (Cieslak et al., 2021), do not have GUI and require users to customize their pipelines by programming, which is challenging for scientific researchers without programming skills. The second set of tools, such as FMRIB Software Library (Smith et al., 2004) (FSL), DiffusionKit (Xie et al., 2016), and Diffusion Toolkit (<http://trackvis.org/dtk/>), do have the GUI but no batch processing pipeline. Users can only process dMRI data step by step or write programs to configure their pipelines. Third, tools such as PANDA (Cui et al., 2013), and Connectome Mapper (Daducci et al., 2012; Tourbier et al., 2022) do have the function of batch processing and GUI, but they do not have the capability to perform network analysis, and PANDA only works on Linux Operating System (OS). Therefore, a ready-for-use pipeline tool without restrictions of specific OS for the construction and analysis of white matter networks is highly desired, especially for users without programming experience.

Moreover, large-scale public datasets, such as UK Biobank (Littlejohns et al., 2020) and HCP (Van Essen et al., 2013), emerge and constantly expand to promote scientific research. Of note, these public datasets have preprocessed neuroimages, especially the fitting of the probabilistic diffusion model for dMRI data, which can be used to reconstruct white matter fibers and then construct networks. Therefore, developing a pipeline using preprocessed dMRI data to construct white matter networks will significantly expedite the research using these datasets.

To simplify the process of human brain network analysis based on dMRI and T1 weighted images, our study aims to develop a reliable, fully automated, cross-platform batch processing toolbox, Diffusion Connectome Pipeline (DCP). DCP provides a friendly GUI that allows

users to choose necessary processing steps and set the processing parameters. DCP can automatically process data of all participants in parallel. It is designed to handle data acquired from MRI scanners with field strengths of 1.5 T or higher and is compatible with both single-shell and multi-shell dMRI data with inclusion of b0 images and more than six diffusion weighted images, in addition to the necessity of T1-weighted images. Its outcomes include different types of weighted matrices and global network metrics such as small world parameters and shortest path length, as well as local network metrics like nodal efficiency and nodal degree centrality. In addition to raw data, the preprocessed probabilistic diffusion model released by these public datasets can be delivered into DCP directly, which saves considerable time by skipping the steps that have been done, especially some time-consuming steps such as eddy current correction and diffusion model estimation. Finally, two validation analyses were carried out on the Beijing Aging Brain Rejuvenation Initiative (BABRI) (Yang et al., 2021) and the HCP (Van Essen et al., 2012) datasets, respectively, to assess the effectiveness of DCP.

## 2 | MATERIALS AND METHODS

DCP was developed based on MATLAB and Docker (<https://www.docker.com/>). MATLAB was used for designing GUI and Docker was used for packaging and running software. The use of Docker makes DCP a cross-platform toolbox. It called toolkits including FSL, Diffusion Toolkit, SPM (<https://www.fil.ion.ucl.ac.uk/spm/>), Camino, MRtrix3, and MRICron (<https://people.cas.sc.edu/rorden/mricron/index.html>). The processing steps in DCP followed by an introduction to the function realization are illustrated in this chapter.

### 2.1 | Overview of the functionality of DCP

The pipeline of DCP includes five steps: (1) preprocessing; (2) tractography; (3) parcellation generation; (4) matrix construction; and (5) network analysis (Figure 1).

#### 2.1.1 | Preprocessing

In this section, to prepare for constructing white matter networks, DCP allows researchers to perform three preprocessing steps that are commonly used in the community: (1) converting DICOM to NIfTI; (2) eddy current, head movement, and susceptibility distortion correction; and (3) diffusion metrics calculation.

*Converting DICOM to NIfTI.* DCP can process both DICOM and NIfTI format as input files. The input files should be organized such that each subject has an individual folder. Within this folder, there should be distinct sub-folders for DTI and T1 files accommodating DICOM or NIfTI formats. The format converting step is skipped when NIfTI images are used as input files. Otherwise, DCP will convert DICOM files to NIfTI files by using the *dcm2nii* tool in MRICron.

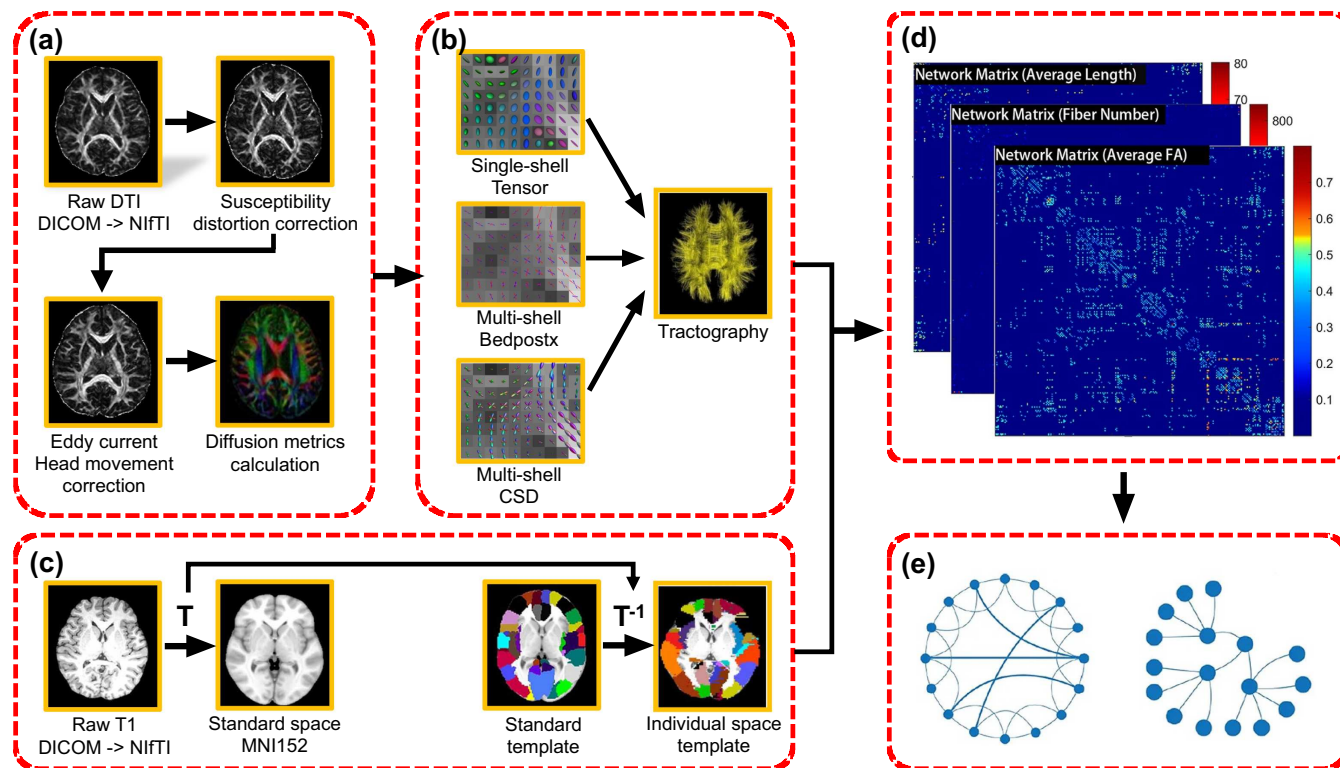


**FIGURE 1** Main procedure for pipeline processing of dMRI datasets in DCP. The procedure includes five parts: (a) preprocessing; (b) performing tractography with single-shell or multi-shell data; (c) parcellating the entire brain into multiple regions where each region represents a network node; (d) constructing networks; and (e) analyzing networks.

*Eddy current, head movement, and susceptibility distortion correction.* Firstly, DCP will decide whether to estimate the field map with *topup* command in FSL according to whether the input data has at least two images with opposite phase encoding directions. Then, DCP combines the correction for susceptibility, eddy currents, and movements by calling *eddy* command in FSL. If the input dMRI data lacks images with opposite phase-encoding directions, only head motion correction, and eddy current correction will be performed. After that, the gradient directions are reoriented based on the transformations of affine alignment (Leemans & Jones, 2009).

*Diffusion metrics calculation.* DCP estimates the diffusion tensor at each voxel in the brain. Based on the diffusion tensor, various measures include fractional anisotropy (FA), mean diffusivity (MD), axial diffusivity, and radial diffusivity are calculated. The *dti\_recon* command in Diffusion Toolkit was called to achieve this function.

### 2.1.2 | Tractography

DCP provides three methods to perform tractography: single-tensor tractography, multi-tensor tractography, and probabilistic tractography based on the constrained spherical deconvolution model.

*Single-tensor tractography.* The diffusion tensor is estimated at each voxel in the brain. The *dti\_recon* command in Diffusion Toolkit was called to achieve this function. Then the fiber assignment by continuous tracking algorithm is used to perform tractography. Every

procedure of the algorithm can be described as follows: (1) select an interested seed zone, and determine the number of seed points per voxel in the seed zone; (2) from a seed point, find the next voxel along with the fiber direction; (3) repeat step (2) until meet a certain stop condition (reaching the gray matter or outside the brain, FA below a threshold value, or mutation of the fiber direction); (4) from the seed point, repeat step (3) along with the opposite direction of the previous track to construct the other half fiber; (5) for each seed point in the seed zone, repeat steps (2)–(4). DCP achieves this by applying the *dti\_tracker* command in Diffusion Toolkit.

*Multi-tensor tractography.* DCP also provides a multi-tensor deterministic tractography method. First, DCP estimates the ball-stick model with the command *bedpostx* from FSL. Then, a multi-tensor fiber tracking algorithm is called to perform tractography. The procedure is almost the same as the above single-tensor fiber tracking algorithm except for step (2), where the fibers enter several different voxels along with different fiber directions because *bedpostx* (Behrens et al., 2003) estimates three fiber directions for each voxel. DCP performs this by using the *track* command in Camino by Docker.

*Probabilistic tractography.* To fully utilize multi-shell data, DCP can perform probabilistic tractography by integrating MRtrix3 into the toolbox. Specifically, DCP estimates the response functions of different tissues using *dwi2response*. Then, fiber orientation distributions are estimated in each voxel based on constrained spherical deconvolution (CSD) model by calling *dwi2fod*. Lastly, *tckgen* is called to perform probabilistic tractography and *tcksift* is called to filter the fiber-tracking data set

such that the streamline densities match the fiber orientation distributions lobe integrals.

### 2.1.3 | Parcellation generation

To define the network nodes, DCP uses prior atlas to divide the entire brain into regions, which are regarded as nodes (Bullmore & Sporns, 2009). Nevertheless, prior atlases defined in the standard space require conversion to the native dMRI space. To complete space conversion, DCP uses the *coregister*, *normalize*, and *deformation* toolbox in SPM. Specifically, the individual structural image (i.e., T1-weighted) is linearly coregistered to its corresponding individual b0 image using the *coregister* toolbox in SPM, and the b0 image is used to estimate the brain mask with the SynthStrip (Hoopes et al., 2022) tool. Then, the mask is used to remove the skull from the individual structure image coregistered to the b0 image space. The individual structure image that is coregistered to the b0 image space is mapped into the ICBM152 template with the *normalize* toolbox in SPM, generating a nonlinear transformation matrix  $T$ . An inverse transformation of  $T$  from the standard space to the native dMRI space is applied to warp prior atlases in the standard space to individual native dMRI space. At present, DCP provides two well-defined atlases: the Automated Anatomical Labeling (AAL) (Tzourio-Mazoyer et al., 2002) atlas and the Brainnetome (BNA) (Fan et al., 2016) atlas. The tractography algorithm can prematurely stop the streamlines in the white matter regions or at the interface between gray matter and white matter. So, the gray matter areas in the two atlases provided by DCP are dilated into white matter. But DCP can also generate fine atlases by multiplying atlases with gray matter mask. Other customized atlases can also be imported into DCP to define the network nodes.

### 2.1.4 | Matrix construction

Two brain regions are considered structurally connected if the weight of connection between them is greater than the given threshold. Based on the attributes of linking fibers, DCP can generate four types of weighted matrices: fiber number (FN)-weighted matrix, FA-weighted matrix, MD-weighted matrix, and length-weighted matrix. Each row or column in the matrix represents a brain region. The value of each element in FN-weighted matrix ( $i, j$ ), FA-weighted matrix ( $i, j$ ), MD-weighted matrix ( $i, j$ ), and length-weighted matrix ( $i, j$ ) represent the fiber number, averaged FA, averaged MD, and averaged length of linking fibers between node  $i$  and node  $j$ , respectively. The resultant matrices are saved as MATLAB data files, which can be directly used for topological analysis, and the text files can be used for checking.

### 2.1.5 | Network analysis

In this section, DCP performs network analyses to calculate various topological properties of a network, including global and nodal

characteristics. Global metrics include small world parameters, clustering coefficient and shortest path length, local efficiency and global efficiency. Local metrics include the nodal clustering coefficient, nodal shortest path length, nodal efficiency, nodal betweenness centrality, nodal degree centrality, and nodal local efficiency. The code for computation of topological properties is from GREYNA (Wang et al., 2015) (<https://github.com/sandywang/GREYNA>), which calculates shortest path length matrix by calling functions from the MatlabBGL toolbox ([https://www.cs.purdue.edu/homes/dgleich/packages/matlab\\_bgl/](https://www.cs.purdue.edu/homes/dgleich/packages/matlab_bgl/)).

## 2.2 | Testing the relationship between structure network metrics and age with DCP

### 2.2.1 | Subjects

A total of 633 cognitively healthy elderly participants which are Han Chinese and right-handed were recruited from the BABRI project (Yang et al., 2021) (age range 45–86 years, mean age  $65.5 \pm 6.9$  years, 393 females). The following inclusion criteria of healthy controls were used: (1) no complaints of memory loss or related disorders causing cognitive impairment; (2) a Clinical Dementia Rating score of 0; (3) Mini-Mental Status Examination (Zhang et al., 1990) score  $\geq 24$ ; and (4) no severe visual or auditory impairment. This study followed the principles of the Declaration of Helsinki and was approved by the Institutional Review Board of the Beijing Normal University Imaging Center for Brain Research. Written informed consent was obtained from each participant.

### 2.2.2 | Image acquisition

The MRI data were acquired with a SIEMENS Trio 3T scanner with a 16-channel phased-array coil at the Imaging Center for Brain Research, Beijing Normal University. All participants underwent high-quality MRI scanning, which included a high-resolution sagittal T1-weighted structural image with a  $1 \text{ mm}^3$  isotropic voxel size: repetition time = 1900 ms, echo time = 87 ms, 176 axial slices, and an axial dMRI image with a  $2 \text{ mm}^3$  isotropic voxel size and 30 diffusion directions:  $b = 1000 \text{ s/mm}^2$ , 1 non-diffusion  $b = 0$  images, repetition time = 9500 ms, echo time = 92 ms, and 70 axial slices.

### 2.2.3 | Image processing

All the dMRI and T1-weighted data were processed with the whole pipeline of DCP to construct FN-weighted structural networks and perform topographic analyses. We set the seed number to 1, turning angle threshold to 45, lower FA threshold to 0.2 when conducting tractography and used the BNA atlas (Fan et al., 2016) to define nodes. Finally, the global efficiency, local efficiency, shortest path length, clustering coefficient, and small-world parameters ( $\lambda$ ,  $\gamma$ , and  $\sigma$ ) were calculated based on graph theory.

## 2.2.4 | Statistical analysis

The relationships between age and brain network metrics were investigated with partial correlation analyses while controlling the effects of gender and years of education. A Bonferroni correction was used for multiple comparisons. The analyses above were performed on MATLAB.

## 2.3 | Testing the test–retest reliability on structure network metrics with DCP

### 2.3.1 | Subjects

The data for this experiment was selected from HCP (Van Essen et al., 2012) including 43 healthy subjects (30 females) aged from 22 to 35 (mean age  $30.3 \pm 3.30$  years). Each subject was scanned twice for dMRI data on two separate days. The intervals between two scanning are from 0.6 to 11.4 months.

### 2.3.2 | Image acquisition

MRI data were collected with a customized 3T Connectome Scanner adapted from Siemens Skyra. T1-weighted scans used 3D magnetization prepared rapid gradient echo (MPRAGE) (slices = 256, TR = 2400 ms, TE = 2.14 ms, flip angle =  $8^\circ$ , and voxel size = 0.7 mm isotropic). A multi-shell diffusion-weighted echo-planar imaging sequence was used for dMRI data (90 diffusion-weighted directions for  $b = 1000, 2000$ , and  $3000$  s/ $\text{mm}^2$  and 18 images with  $b = 0$  s/ $\text{mm}^2$ , slices = 111, TR = 5500 ms, TE = 89.50 ms, slice thickness = 1.25 mm, FOV =  $210 \times 180$   $\text{mm}^2$ , and acquisition matrix =  $168 \times 144$ ).

### 2.3.3 | Image processing

The HCP dataset provides resultant files after being processed by bedpost (Behrens et al., 2003). Those files were directly put into DCP to execute tractography. We used the BNA atlas (Fan et al., 2016) to define nodes and constructed FN-weighted networks. Finally, global efficiency, local efficiency, shortest path length, clustering coefficient, and small-world parameters ( $\lambda$ ,  $\gamma$ , and  $\sigma$ ) were calculated for each network.

### 2.3.4 | Statistical analysis

The intraclass coefficient (ICC) (Shrout & Fleiss, 1979) and Pearson correlation were used to evaluate the test–retest reliability of the network metrics between two sessions. The ICC was calculated as follows:

$$\text{ICC} = \frac{\sigma_{\text{bs}}^2 - \sigma_{\text{ws}}^2}{\sigma_{\text{bs}}^2 + (m-1)\sigma_{\text{ws}}^2} \quad (1)$$

where  $\sigma_{\text{bs}}$  is the between-subject variance,  $\sigma_{\text{ws}}$  is the within-subject variance, and  $m$  represents the number of repeated measurements.

ICC is a normalized measure and ranges from 0 to 1. Normally, ICC values can be separated into five common intervals (Landis & Koch, 1977):  $0 < \text{ICC} \leq 0.2$  (slight),  $0.2 < \text{ICC} \leq 0.4$  (fair),  $0.4 < \text{ICC} \leq 0.6$  (moderate),  $0.6 < \text{ICC} \leq 0.8$  (substantial), and  $0.8 < \text{ICC} \leq 1.0$  (almost perfect).

## 3 | RESULTS

### 3.1 | An integrative MATLAB toolbox: DCP

We developed DCP, an integrative MATLAB toolbox for processing dMRI data, constructing structural network, and performing network analysis. It not only provides batch processing but can also be executed separately for a single step (e.g., preprocessing, tractography, parcellation generation, matrix construction, and network analysis). In addition, DCP has a friendly GUI (Figure 2), providing options for necessary steps and detail setting, allowing users to perform processing tasks according to personalized requirement, for example, setting the processing parameters and path of the output file. Besides, users can get the real-time status of the program running from the GUI of DCP. Once the program finishes, the parcellation in native space will be saved as a PNG picture for users to check whether there is any error in the process of generating parcellation.

### 3.2 | Resultant files of DCP

First, DCP generates three folders for each subject (Table 1). Specifically, the *DTI\_DATA* folder consists of resultant files of preprocess and tractography. The *PARCELLATION* folder includes the resultant files of parcellation. The *MATRIX* folder contains the matrix files of constructed network. Then, output folder will be generated in the parent directory of the input folder if users do not specify one. It contains a folder named QC, which consists of quality control files (Figure 3) of all the subjects and a MATLAB file that contains networks of all subjects. Finally, output folder of network analysis will be generated in the specified path, which contains each folder for each network matrix constructed with specific parameters. Within the folders, each network property has a MATLAB file containing metrics of all subjects.

### 3.3 | Performance of DCP

Use of the Parallel Computing Toolbox in MATLAB enables DCP to process data in parallel. To investigate the efficiency of DCP in processing image data, we conducted a few baseline running-time tests based on the BABRI and HCP datasets. The time cost of constructing structural networks for different numbers of subjects (1, 2, 10, 30)

### Diffusion Connectome Pipeline (DCP)

**DataPath**  **Select** All subjects Parallel

**PreProcess**

Convert  Eddy correct  Tensor calculation

Acquisition parameter  **Select** Acquisition index  **Select**

**Brain Parcellation**

Template  **Select**  GM mask

AAL 90  BNA 246 Other Atlas  **Select**

**Fiber Tractography**

FA threshold  Turn angle

Seed number  Invert  Swap

**Network Construction**

Weight  FN  FA  MD  Length

**Merge**  **Select**

**Network Analysis**

Global

Small-World  Global Efficiency  Rich-Club

Nodal

Clustering Coefficient  Shortest Path Length  Nodal efficiency

Betweenness Centrality  Degree Centrality  Local Efficiency

**OutputPath**  **Select**

**Default** **Save** **Load** Run

**FIGURE 2** A snapshot of the GUI of DCP. The GUI allows for inputting raw dMRI datasets or the datasets processed by *bedpostx* and configuring the processing parameters and monitoring the progress of data processing in real-time.

**TABLE 1** Folders produced by DCP.

Folder name	Files
DTI_DATA	Resultant files of preprocess and tractography
PARCELLATION	Resultant files of generating parcellation
MATRIX	Resultant files of constructing network
QC	Resultant files of quality control

**TABLE 2** Baseline time cost of pipeline processing on raw dataset with DCP.

	Time cost (min)		
	1 subject	10 subjects	30 subjects
Single tensor	41	61	119
Multiple tensor	73	95	188
Probabilistic tractography	69	89	176

was recorded. In the BABRI dataset, a single-tensor fiber tracking algorithm based on the original data was used. In the HCP dataset, the structural network was constructed using a multi-tensor fiber tracking algorithm with the data processed by *bedpost* (Behrens

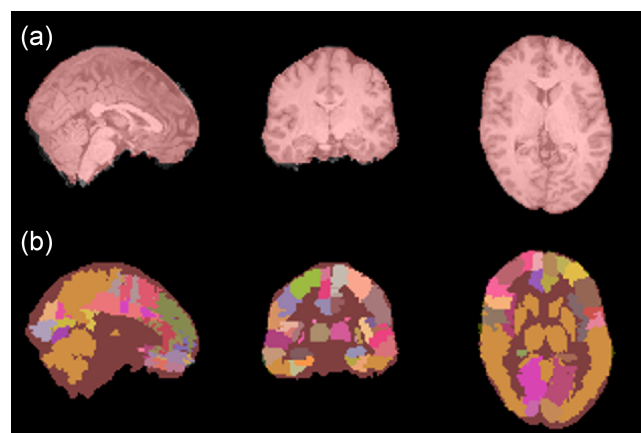


**FIGURE 3** Quality control for the preprocessing. (a) The b0 mask (red) was overlaid on the T1 image (gray) that was coregistered to the native dMRI space, and (b) the b0 mask (red) was overlaid on the native parcellation atlas (gray). These pictures can be quickly viewed to check the quality of registration and normalization.

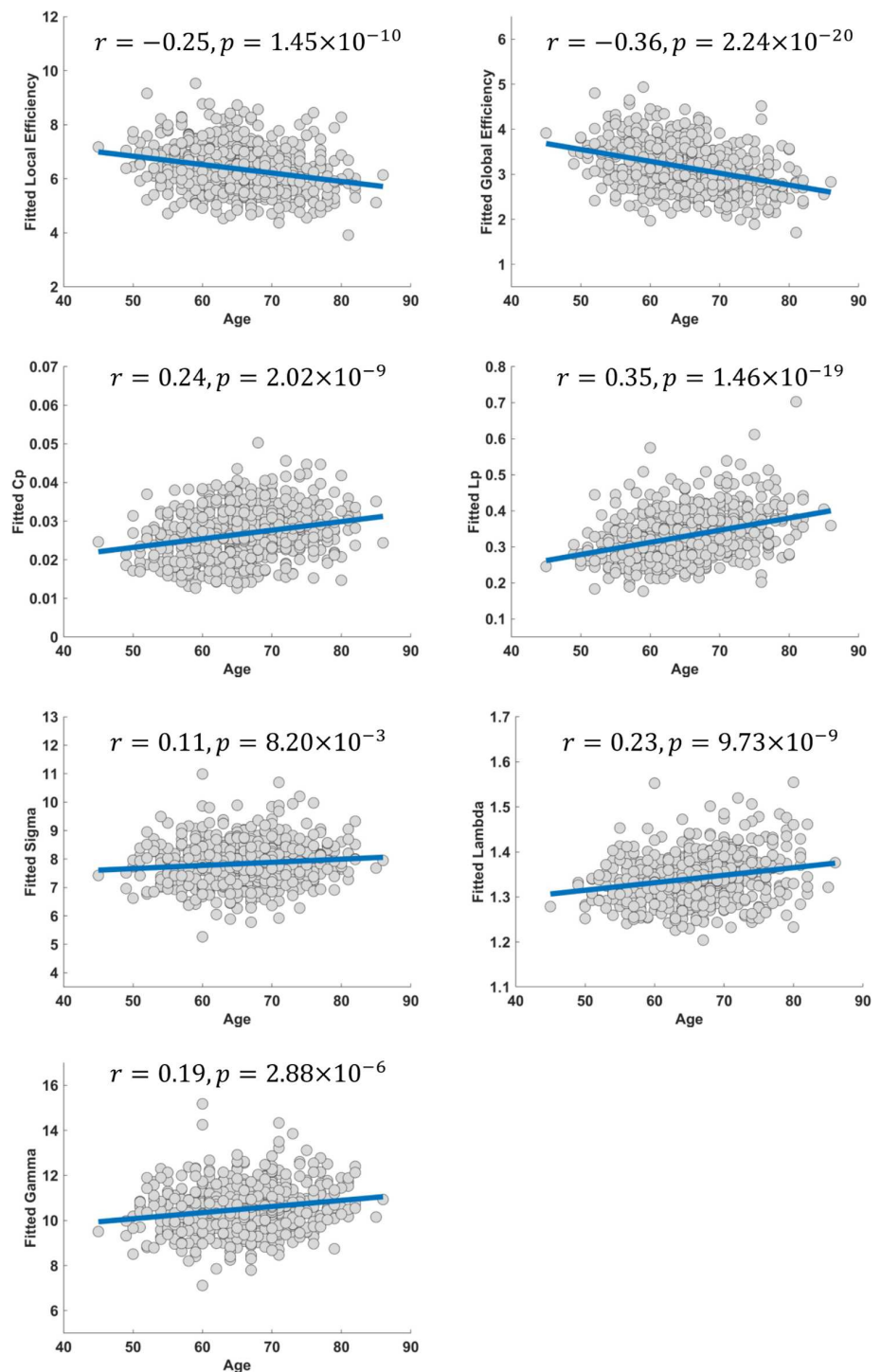
et al., 2003). As shown in Table 2, the time consumption of the whole pipeline using single-tensor fiber tracking and multi-tensor fiber tracking algorithms was reported.

### 3.4 | The correlation between age and network metrics with DCP

As shown in Figure 4, with increasing age, the participants showed significant decreases in local efficiency ( $r = -0.25, p = 1.45 \times 10^{-10}$ ) and global efficiency ( $r = -0.36, p = 2.24 \times 10^{-20}$ ) and significant increases in the clustering coefficient ( $r = 0.24, p = 2.02 \times 10^{-9}$ ), shortest path length ( $r = 0.35, p = 1.46 \times 10^{-19}$ ), sigma ( $r = 0.11, p = 8.2 \times 10^{-3}$ ), lambda ( $r = 0.23, p = 9.73 \times 10^{-9}$ ), and gamma ( $r = 0.19, p = 2.88 \times 10^{-6}$ ).

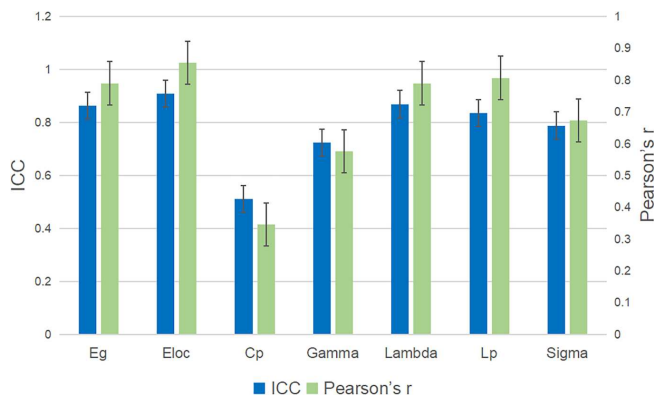
### 3.5 | The test-retest reliability on structure network metrics with DCP

Figure 5 showed the test-retest reliability on graph metrics of dMRI data processed with DCP. Global efficiency (ICC = 0.86,  $r = 0.79$ ), local efficiency (ICC = 0.91,  $r = 0.86$ ), shortest path length (ICC = 0.84,  $r = 0.81$ ), sigma (ICC = 0.79,  $r = 0.67$ ), lambda (ICC = 0.87,  $r = 0.79$ ), and gamma (ICC = 0.72,  $r = 0.58$ ) showed high reliability. Only the clustering coefficient (ICC = 0.51,  $r = 0.35$ ) showed moderate reliability.



**FIGURE 4** Age effects on network topological properties. The fitted values indicate the residuals of the original values of the network metrics after removing the effects of gender and years of education. All these global topological properties showed significant alterations with age. Cp, clustering coefficient; Lp, shortest path length.





**FIGURE 5** The test-retest reliability of global network properties. The bars and error bars respectively represent the mean and standard deviations of ICC and Pearson correlation. Cp, clustering coefficient; Eg, global efficiency; Eloc, local efficiency; ICC, intra-class coefficient; Lp, shortest path length.

## 4 | DISCUSSION

In this study, we developed a MATLAB toolbox named DCP to construct brain structural networks and calculated the topological properties of networks using raw dMRI data automatically. The toolbox can be used on Windows, Linux, and Mac OS, with a friendly GUI, which allows users to configure a processing pipeline without programming. DCP offers users a range of diffusion tensor estimation and fiber tracking methods, allowing them to choose based on the specific characteristics of their data. And DCP is very flexible, not only processing raw dMRI data to the last step but also being executed separately for specific processing steps. Particularly, DCP can use the processed data from most well-known datasets as direct input, which saves considerable time by skipping the steps that have already been performed. Furthermore, parallel computation is supported to significantly reduce the time cost of the pipeline.

To evaluate the validity of DCP, we applied it to explore the age effects on topological metrics of structural networks generated by DCP. We found significant decreases in global efficiency and local efficiency as well as increase in shortest path length, clustering coefficient and small-world parameters (lambda, gamma, and sigma) with increasing age. These findings reproduced the conclusions that were found in our previous studies (Li et al., 2020; Zhao et al., 2015). In addition, we applied DCP to the HCP dataset to assess the test-retest reliability of white matter networks. All topological metrics except the cluster coefficient showed high reliability. The ICC values obtained are comparable with the findings of previous studies (Bassett et al., 2011; Buchanan et al., 2014; Cheng et al., 2012; Vaessen et al., 2010; Zhao et al., 2015). These two experiments demonstrate that DCP is effective.

In particular, typical dMRI processing involves more than 10 steps, each with specific parameters and potentially relying on different neuroimaging toolboxes. The processing procedures from different existing software packages differ slightly. DCP tries to use rational procedures as much as possible. For instance, DCP provides CSD

method for intravoxel reconstruction with multi-shell data. CSD excels at resolving complex fiber configurations and is particularly effective in regions with fiber crossings. It is an advanced technique providing more accurate estimates of multiple fiber orientations within a voxel. In addition, DCP incorporates an innovative tool, SynthStrip, known for its robust and accurate skull stripping capabilities. This tool employs a deep learning strategy to synthesize arbitrary training images from segmentation maps, resulting in a robust model that is agnostic to acquisition specifics. In the future, DCP will continue to be updated to include the most advanced procedures.

There are several limitations of DCP need to be addressed in the future. First, DCP can only construct and analyze white matter networks weighted based on tensor-derived metrics but not the advanced metrics such as fixel-based metrics, which provide a more detailed and nuanced view of white matter microstructure. Second, relying on MATLAB, which is restricted access and expensive, is not friendly to users.

In summary, we developed a user-friendly toolbox, DCP, to provide researchers with measures for white matter connections and network analysis based on dMRI and T1 weighted images. We hope it will contribute to facilitating and standardizing human connectome studies in the near future.

## ACKNOWLEDGEMENTS

WJH's participation is funded by the STI2030-Major Projects (grant no. 2022ZD0213300), National Natural Science Foundation of China (grant nos. 2231200165, 210510238), and China Scholarship Council. NS's participation is funded by the STI2030-Major Projects (grant nos. 2022ZD0213300, 2021ZD0200500), National Natural Science Foundation of China (grant nos. 32271145, 81871425), Fundamental Research Funds for the Central Universities (grant no. 2017XTCX04), Open Research Fund of the State Key Laboratory of Cognitive Neuroscience and Learning (grant nos. CNLZD2101, CNLYB2001).

## CONFLICT OF INTEREST STATEMENT

There are no conflicts of interest including any financial, personal, or other relationships with people or organizations for any of the authors related to the work described in the article.

## DATA AVAILABILITY STATEMENT

The data that support the findings of this study are available on request from the corresponding author. The data are not publicly available due to privacy or ethical restrictions.

## ORCID

Weijie Huang  <https://orcid.org/0000-0002-2481-1188>

## REFERENCES

- Bassett, D. S., Brown, J. A., Deshpande, V., Carlson, J. M., & Grafton, S. T. (2011). Conserved and variable architecture of human white matter connectivity. *NeuroImage*, 54, 1262–1279.
- Behrens, T. E., & Sporns, O. (2012). Human connectomics. *Current Opinion in Neurobiology*, 22, 144–153.

- Behrens, T. E. J., Woolrich, M. W., Jenkinson, M., Johansen-Berg, H., Nunes, R. G., Clare, S., Matthews, P. M., Brady, J. M., & Smith, S. M. (2003). Characterization and propagation of uncertainty in diffusion-weighted MR imaging. *Magnetic Resonance in Medicine*, *50*, 1077–1088.
- Buchanan, C. R., Pernet, C. R., Gorgolewski, K. J., Storkey, A. J., & Bastin, M. E. (2014). Test–retest reliability of structural brain networks from diffusion MRI. *NeuroImage*, *86*, 231–243.
- Bullmore, E., & Sporns, O. (2009). Complex brain networks: Graph theoretical analysis of structural and functional systems. *Nature Review Neuroscience*, *10*, 186–198.
- Cheng, H., Wang, Y., Sheng, J., Kronenberger, W. G., Mathews, V. P., Hummer, T. A., & Saykin, A. J. (2012). Characteristics and variability of structural networks derived from diffusion tensor imaging. *NeuroImage*, *61*, 1153–1164.
- Cieslak, M., Cook, P. A., He, X., Yeh, F. C., Dhollander, T., Adebimpe, A., Aguirre, G. K., Basset, D. S., Betzel, R. F., Bourque, J., Cabral, L. M., Davatzikos, C., Detre, J. A., Earl, E., Elliott, M. A., Fadnavis, S., Fair, D. A., Foran, W., Fotiadis, P., ... Satterthwaite, T. D. (2021). QSI-Prep: An integrative platform for preprocessing and reconstructing diffusion MRI data. *Nature Methods*, *18*, 775–778.
- Cook, P., Bai, Y., Hall, M. G., Nedjati-Gilani, S., Seunarine, K. K., & Alexander, D. C. (2006). Camino: Open-Source Diffusion MRI reconstruction and processing. *14th Scientific Meeting of the International Society for Magnetic Resonance in Medicine*, 2759.
- Cui, Z., Zhong, S., Xu, P., He, Y., & Gong, G. (2013). PANDA: A pipeline toolbox for analyzing brain diffusion images. *Frontiers in Human Neuroscience [Online Serial]*, *7*, 42. <https://doi.org/10.3389/fnhum.2013.00042/abstract>
- Daducci, A., Gerhard, S., Griffa, A., Lemkaddem, A., Cammoun, L., Gigandet, X., Meuli, R., Hagmann, P., & Thiran, J. P. (2012). The connectome mapper: An open-source processing pipeline to map connectomes with MRI. *PLoS One*, *7*, e48121.
- Descoteaux, M., Deriche, R., Knosche, T. R., & Anwander, A. (2009). Deterministic and probabilistic tractography based on complex fibre orientation distributions. *IEEE Transactions on Medical Imaging*, *28*, 269–286.
- Fan, L., Li, H., Zhuo, J., Zhang, Y., Wang, J., Chen, L., Yang, Z., Chu, C., Xie, S., Laird, A. R., Fox, P. T., Eickhoff, S. B., Yu, C., & Jiang, T. (2016). The human Brainnetome atlas: A new brain atlas based on connective architecture. *Cerebral Cortex*, *26*, 3508–3526.
- Fornito, A., Zalesky, A., & Breakspear, M. (2015). The connectomics of brain disorders. *Nature Reviews Neuroscience*, *16*, 159–172.
- Garyfallidis, E., Brett, M., Amirbekian, B., Rokem, A., van der Walt, S., Descoteaux, M., Nimmo-Smith, I., & Dipy Contributors. (2014). Dipy, a library for the analysis of diffusion MRI data. *Frontiers in Neuroinformatics [Online Serial]*, *8*, 8. <https://doi.org/10.3389/fninf.2014.00008>
- Girard, G., Whittingstall, K., Deriche, R., & Descoteaux, M. (2014). Towards quantitative connectivity analysis: Reducing tractography biases. *NeuroImage*, *98*, 266–278.
- Hoopes, A., Mora, J. S., Dalca, A. V., Fischl, B., & Hoffmann, M. (2022). SynthStrip: Skull-stripping for any brain image. *NeuroImage*, *260*, 119474.
- Landis, J., & Koch, G. (1977). Measurement of observer agreement for categorical data. *Biometrics*, *33*, 159–174.
- Leemans, A., & Jones, D. K. (2009). The B-matrix must be rotated when correcting for subject motion in DTI data. *Magnetic Resonance in Medicine*, *61*, 1336–1349.
- Li, X., Wang, Y., Wang, W., Huang, W., Chen, K., Xu, K., Zhang, J., Chen, Y., Li, H., Wei, D., Shu, N., & Zhang, Z. (2020). Age-related decline in the topological efficiency of the brain structural connectome and cognitive aging. *Cerebral Cortex*, *30*, 4651–4661.
- Littlejohns, T. J., Holliday, J., Gibson, L. M., Garratt, S., Oesingmann, N., Alfaro-Almagro, F., Bell, J. D., Boultonwood, C., Collins, R., Conroy, M. C., Crabtree, N., Doherty, N., Frangi, A. F., Harvey, N. C., Leeson, P., Miller, K. L., Neubauer, S., Petersen, S. E., Sellors, J., ... Allen, N. E. (2020). The UK biobank imaging enhancement of 100,000 participants: Rationale, data collection, management and future directions. *Nature Communications*, *11*, 2624.
- Passingham, R. E., Stephan, K. E., & Kötter, R. (2002). The anatomical basis of functional localization in the cortex. *Nature Reviews Neuroscience*, *3*, 606–616.
- Shrout, P. E., & Fleiss, J. L. (1979). Intraclass correlations: Uses in assessing rater reliability. *Psychological Bulletin*, *86*, 420–428.
- Smith, S. M., Jenkinson, M., Woolrich, M. W., Beckmann, C. F., Behrens, T. E. J., Johansen-Berg, H., Bannister, P. R., de Luca, M., Drobnjak, I., Flitney, D. E., Niazy, R. K., Saunders, J., Vickers, J., Zhang, Y., de Stefano, N., Brady, J. M., & Matthews, P. M. (2004). Advances in functional and structural MR image analysis and implementation as FSL. *NeuroImage*, *23*, S208–S219.
- Sporns, O. (2011). The human connectome: A complex network. *Annals of the New York Academy of Sciences*, *1224*, 109–125.
- Tourbier, S., Rue-Queralt, J., Glomb, K., Aleman-Gomez, Y., Mullier, E., Griffa, A., Schöttner, M., Wirsich, J., Tuncel, M. A., Jancovic, J., Cuadra, M. B., & Hagmann, P. (2022). Connectome mapper 3: A flexible and open-source pipeline software for multiscale multimodal human connectome mapping. *Journal of Open Source Software*, *7*, 4248.
- Tournier, J.-D., Smith, R., Raffelt, D., Tabbara, R., Dhollander, T., Pietsch, M., Christiaens, D., Jeurissen, B., Yeh, C. H., & Connelly, A. (2019). MRtrix3: A fast, flexible and open software framework for medical image processing and visualisation. *NeuroImage*, *202*, 116137.
- Tzourio-Mazoyer, N., Landeau, B., Papathanassiou, D., Crivello, F., Etard, O., Delcroix, N., Mazoyer, B., & Joliot, M. (2002). Automated anatomical labeling of activations in SPM using a macroscopic anatomical parcellation of the MNI MRI single-subject brain. *NeuroImage*, *15*, 273–289.
- Vaessen, M. J., Hofman, P. a. M., Tijssen, H. N., Aldenkamp, A. P., Jansen, J. F. A., & Backes, W. H. (2010). The effect and reproducibility of different clinical DTI gradient sets on small world brain connectivity measures. *NeuroImage*, *51*, 1106–1116.
- van den Heuvel, M. P., & Sporns, O. (2019). A cross-disorder connectome landscape of brain dysconnectivity. *Nature Reviews Neuroscience*, *20*, 435–446.
- Van Essen, D. C., Smith, S. M., Barch, D. M., Behrens, T. E. J., Yacoub, E., & Ugurbil, K. (2013). The WU-Minn human connectome project: An overview. *NeuroImage*, *80*, 62–79.
- Van Essen, D. C., Ugurbil, K., Auerbach, E., Barch, D., Behrens, T. E. J., Bucholz, R., Chang, A., Chen, L., Corbetta, M., Curtiss, S. W., Penna, S. D., Feinberg, D., Glasser, M. F., Harel, N., Heath, A. C., Larson-Prior, L., Marcus, D., Michalareas, G., Moeller, S., ... WU-Minn HCP Consortium. (2012). The human connectome project: A data acquisition perspective. *NeuroImage*, *62*, 2222–2231.
- Wang, J., Wang, X., Xia, M., Liao, X., Evans, A., & He, Y. (2015). GREYNA: A graph theoretical network analysis toolbox for imaging connectomics. *Frontiers in Human Neuroscience*, *9*, 386.
- Xie, S., Chen, L., Zuo, N., & Jiang, T. (2016). DiffusionKit: A light one-stop solution for diffusion MRI data analysis. *Journal of Neuroscience Methods*, *273*, 107–119.
- Yang, C., Li, X., Zhang, J., Chen, Y., Li, H., Wei, D., Lu, P., Liang, Y., Liu, Z., Shu, N., Wang, F., Guan, Q., Tao, W., Wang, Q., Jia, J., Ai, L., Cui, R., Wang, Y., Peng, D., ... Beijing Aging Brain Rejuvenation Initiative workgroup. (2021). Early prevention of cognitive impairment in the community population: The Beijing Aging Brain Rejuvenation Initiative. *Alzheimer's & Dementia*, *17*(10), 1610–1618.
- Zhang, M. Y., Katzman, R., Salmon, D., Jin, H., Cai, G., Wang, Z., Qu, G., Grant, I., Yu, E., Levy, P., Klauber, M. R., & Liu, W. T. (1990). The prevalence of dementia and Alzheimer's disease in Shanghai, China: Impact of age, gender, and education. *Annals of Neurology*, *27*, 428–437.
- Zhao, T., Cao, M., Niu, H., Zuo, X. N., Evans, A., He, Y., Dong, Q., & Shu, N. (2015). Age-related changes in the topological organization of the

white matter structural connectome across the human lifespan. *Human Brain Mapping*, 36, 3777–3792.

Zhao, T., Duan, F., Liao, X., Dai, Z., Cao, M., He, Y., & Shu, N. (2015). Test–retest reliability of white matter structural brain networks: A multiband diffusion MRI study. *Frontiers in Human Neuroscience [Online Serial]*, 9, 59. <https://doi.org/10.3389/fnhum.2015.00059/abstract>

**How to cite this article:** Huang, W., Dong, X., Zhao, T., Kucikova, L., Fu, A., & Shu, N. (2024). DCP: A pipeline toolbox for diffusion connectome. *Human Brain Mapping*, 45(3), e26626. <https://doi.org/10.1002/hbm.26626>